Nanoscale

COMMUNICATION

View Article Online
View Journal | View Issue

Cite this: *Nanoscale*, 2016, **8**, 4475

Received 15th October 2015,
Accepted 14th January 2016

DOI: 10.1039/c5nr07155k

www.rsc.org/nanoscale

Probing the PEDOT:PSS/cell interface with conductive colloidal probe AFM-SECM†

P. Knittel,[a] H. Zhang,[b] C. Kranz,*[a] G. G. Wallace[b] and M. J. Higgins*[b]

Conductive colloidal probe Atomic Force-Scanning Electrochemical Microscopy (AFM-SECM) is a new approach, which employs electrically insulated AFM probes except for a gold-coated colloid located at the end of the cantilever. Hence, force measurements can be performed while biasing the conductive colloid under physiological conditions. Moreover, such colloids can be modified by electrochemical polymerization resulting, *e.g.* in conductive polymer-coated spheres, which in addition may be loaded with specific dopants. In contrast to other AFM-based single cell force spectroscopy measurements, these probes allow adhesion measurements at the cell–biomaterial interface on multiple cells in a rapid manner while the properties of the polymer can be changed by applying a bias. In addition, spatially resolved electrochemical information *e.g.*, oxygen reduction can be obtained simultaneously. Conductive colloid AFM-SECM probes modified with poly(3,4-ethylenedioxythiophene) doped with polystyrene sulfonate (PEDOT:PSS) are used for single cell force measurements in mouse fibroblasts and single cell interactions are investigated as a function of the applied potential.

The interface between living cells and functional materials is the focus of intensive research in an attempt to understand adhesion, spreading, migration, proliferation and differentiation of cells. Among functional materials, conductive polymers such as poly-3,4-ethylenedioxythiophene (PEDOT) and polypyrrole (PPy) are promising substrates for cell growth as properties like topography, surface chemistry, conductivity, and stiffness of the polymer can be easily tuned.[1] The stability of PEDOT and in particular of PEDOT:PSS renders this conductive polymer also interesting as a scaffold material.[2] Marzocchi *et al.* recently investigated cell growth on PEDOT:PSS and its dependence on the physical and chemical properties.[3] It was shown that the cell proliferation not only depends on the cell type, but also on the redox state of the polymer as well as the fabrication method of the PEDOT. Hence, studying the adhesion of cells and characterizing the cell–PEDOT interface at a single cell level is a prerequisite to understand cell functions when in contact with the polymer. Yet, little is known about the physical interactions such as adhesion mechanisms at the single cell and molecular level and how they are affected by changes in electrically controlled redox properties.

Here, we present a novel approach for studying cell adhesion at the single cell level using conductive colloidal AFM-SECM probes coated with PEDOT:PSS. The fabrication process of such probes is described and the capability of simultaneously performing force and electrochemical measurements on model samples as well as live cells is demonstrated. Cell adhesion is frequently determined with washing assays and shear force measurements,[4,5] alternatively, single-molecule force spectroscopy (SMFS) has gained considerable interest for probing molecular-level interactions.[6] SMFS includes optical and magnetic tweezers, atomic force microscopy (AFM), microneedles and pressurized microcapsules that allow for the detection of biomolecular and cellular adhesion in a force range of 0.1–100 pN (optical tweezers) to $10–10^4$ pN (AFM) with high temporal and spatial resolution.[7–9] In particular, AFM is an attractive technique, enabling 3D-mapping and quantitative analysis of single receptor–ligand bonds across the surface of living cells over a wide range of detectable forces.[10]

Several limitations of AFM-based SMFS such as high mechanical stress exerted on cells, reduced probability of binding, and increased susceptibility to fouling of the tip are avoided with single-cell force spectroscopy (SCFS) that involves attaching a single living cell onto a tipless AFM cantilever.[11] SCFS allows the quantification of single receptor binding, focal adhesion clusters and whole cell adhesion. These important insights characterizing single cell adhesion obtained by SCFS have come at the expense of labor-intensive preparation of the live cell-modified AFM cantilevers, low-throughput and limited

[a]University of Ulm, Institute of Analytical and Bioanalytical Chemistry, Albert-Einstein-Allee 11, 89081 Ulm, Germany. E-mail: christine.kranz@uni-ulm.de
[b]ARC Centre of Excellence for Electromaterials Science, Intelligent Polymer Research Institute, University of Wollongong, Wollongong, 2522, Australia.
E-mail: mhiggins@uow.edu.au

†Electronic supplementary information (ESI) available. See DOI: 10.1039/c5nr07155k

measurement numbers due to cell viability.[12] Most SCFS studies to date have focused on measuring cell adhesion forces on extracellular matrix components (*e.g.* collagen, fibronectin),[13] although SCFS has recently been shown to be highly suited for quantifying cell adhesion on materials such as synthetic polymers, biomaterials and stimuli-responsive surfaces. For example, SCFS has been applied to study cell adhesion on protein repellent polymer coatings and electrically switchable polymers.[14,15] We recently demonstrated that combined AFM-Scanning Electrochemical Microscopy (SECM) probes with nanoscopic PPy electrodes are highly suitable for adhesion measurements under potential control. It was shown that such probes enable electrical stimulation of living cells and force measurements on model samples depending on the applied potential.[16] However, the probes utilize a nanoscale tip and therefore suffer from similar limitations as SMFS.

Colloidal probe AFM has become an important tool for studying force interactions, adhesion and mechanics of cells with a broad variety of substrates including nanostructured materials.[17,18] The increased contact area of a micron-sized colloidal probe drastically decreases the mechanical pressure and multiple cells can be measured with a single probe. However, this approach is limited, as coating of the silica probe with the material of interest may be challenging.

Here, we introduce "Conductive Colloidal Probe AFM-SECM" that adopts the advantages of both SMFS and SCFS, namely the detection of whole cell adhesion and molecular level forces with high throughput under potentiostatic control. The cantilever is entirely insulated except the gold-coated sphere, which is electrically connected; hence a colloidal electrode suitable for electrochemical experiments is obtained. This facilitates electrophoretic induced deposition, and/or specific surface functionalization, enabling the deposition of material coatings onto the colloidal probe for exploring a range of cell–electrode material interactions, which is currently of significant interest.[19]

Fabrication methods developed for AFM-SECM probes with different geometries include conical electrodes,[20] integrated frame electrodes,[21] or handmade cantilever-shaped sub-micrometer spherical gold electrodes.[22] For obtaining a conductive colloidal probe, the attachment of a colloid and subsequent application of a metallic coating would be feasible.[23] However, for measurements under physiological conditions, an important aspect is complete insulation of the cantilever. The selective, reproducible removal of an insulating layer solely from a spherical particle is rather challenging, *e.g.*, using chemical etching or FIB milling. The conductive colloidal probes are fabricated using commercially available soft cantilevers, which are coated with Ti/Au on the frontside, followed by insulation *via* plasma-enhanced chemical vapor deposition (PECVD) with mixed layers of silicon nitride/silicon dioxide (Si_xN_y/SiO_2) (Fig. 1a and Fig. S1†). Gas-assisted focused ion beam (FIB)-milling using xenon difluoride (XeF_2) was used for selectively removing the insulation layer exposing an inlaid disc-shaped electrode (Fig. 1b). As the conductive colloids have a diameter of 5.02 ± 0.12 μm, a gold area of 4 μm in diameter was exposed using the endpoint monitor function to control the milling depth (Fig. S1b–d†). Following protocols for colloid attachment,[24] a gold-coated polystyrene colloid was glued to the exposed conductive area of the cantilever using a non-conductive UV curable glue, which allowed attachment but did not completely coat (insulate) the inlaid disc electrode (Fig. 1c). The electrical contact was made at an exposed contact pad on the AFM chip with conductive epoxy glue and the contact was subsequently insulated with UV glue.

To characterize the individual fabrication steps, cyclic voltammograms (CVs) were recorded in hexaammineruthenium(III) chloride/potassium chloride ($[Ru(NH_3)_6]Cl_3$/0.1 M KCl) (Fig. 1e and Fig. S2a†). After attachment of the conductive colloid, a significant increase in current is visible, indicating a perfect electrical contact (red-solid *vs.* blue-dashed trace). Due to the micro-sized dimension of the electrode, the obtained faradaic current is not limited by mass transport and the steady-state current can be used to calculate the diameter of the disc-shaped and spherical microelectrode with the following equations:[25,26]

$$i_{ss} = 4nFDc_0r_0 \ \text{(disc)} \tag{1}$$

$$i_{ss} = 4\pi nFDc_0r_0 \ \text{(sphere)} \tag{2}$$

with a diffusion constant for the redox species $D = 5.3 \times 10^{-6}$ $cm^2\ s^{-1}$,[26] the Faraday constant F, the number of electrons transferred ($n = 1$), and the bulk concentration c_0.

The obtained steady-state current i_{ss} is 5 nA (Fig. 1e, blue dashed line) for the probe as shown in Fig. 1b. Based on eqn (1), the resulting electrode radius r_0 is 2.44 μm, which is in good agreement with the radius of the inlaid disc electrode obtained from SEM (Fig. 1b), taking the roughness of the gold layer into account. For the colloid shown in Fig. 1c, the recorded reduction current at −250 mV *vs.* Ag/AgCl is −17 nA (Fig. 1e, red trace). Using eqn (2), a radius of 2.65 μm and hence a diameter for the conductive colloid of 5.3 μm is determined, which is in excellent agreement with the diameter obtained from the SEM image (Fig. 1c).

PEDOT:PSS was subsequently electrochemically deposited onto the colloid *via* CV using 10 cycles with a potential window from −0.6 V to 1 V (*vs.* Ag/AgCl).[27] The electropolymerization was terminated at a negative potential, resulting in a partially reduced state of the polymer. Due to the electrical conductivity of PEDOT:PSS, the deposition and resulting increase in the electroactive surface area can be followed by the rising current in each subsequent potential cycle (Fig. S2b†). The deposition process resulted in a complete coverage of the colloid with the polymer, exhibiting characteristic "cauliflower" morphology, as well as preserving the overall spherical geometry of the probe (Fig. 1d). A FIB cross section of the coated colloid revealed a polymer layer thickness of approximately 1 μm. Additionally, energy dispersive X-ray (EDX) spectra recorded at the colloid core (red circle) and the deposited polymer layer (blue circle) were recorded (Fig. 1f). The EDX spectra of the PEDOT:PSS (blue spectra) layer show sulphur (S Kα) and sodium (Na Kα) peaks, which is expected

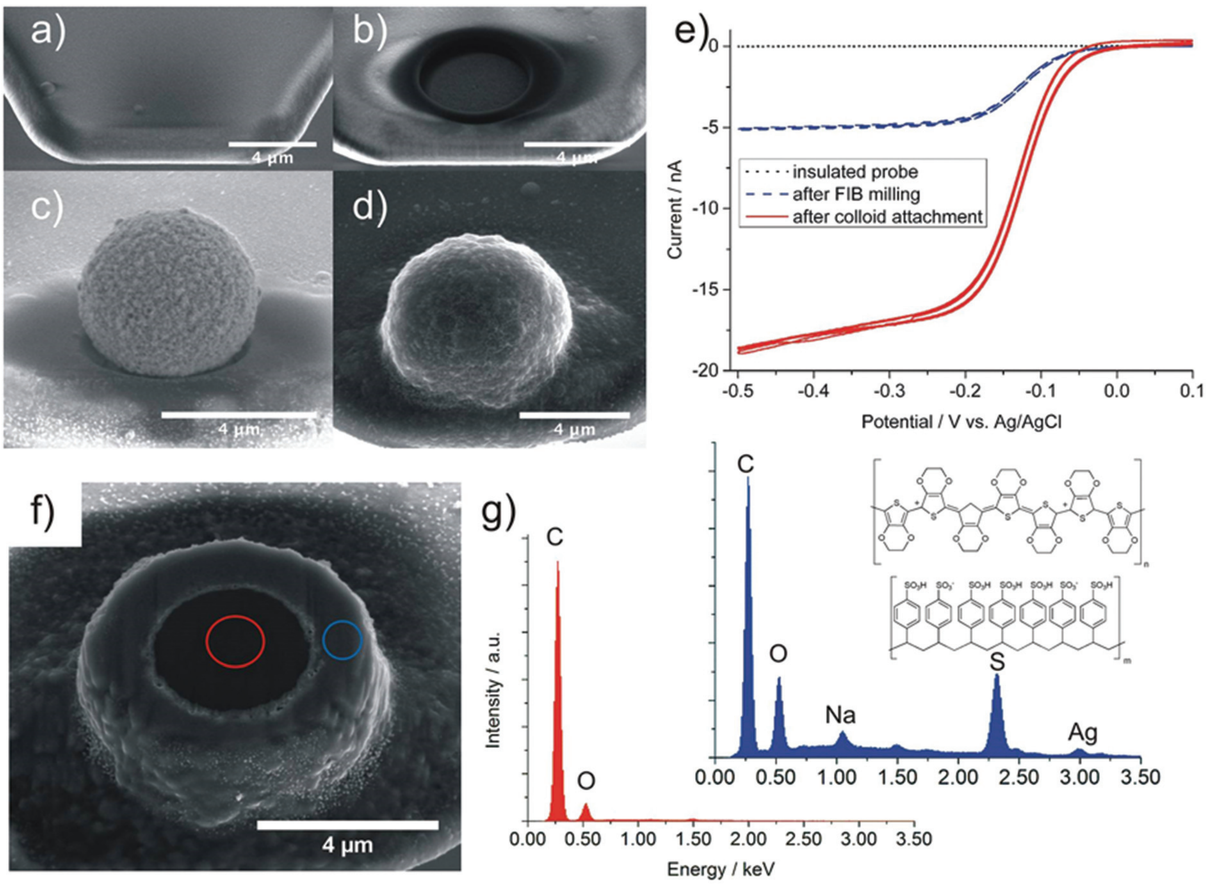

Fig. 1 Fabrication of the PEDOT:PSS-coated conductive colloidal AFM-SECM probe. (a–d) SEM images of the main fabrication steps (insulation, milling, colloid attachment and polymer deposition). (e) Electrochemical characterization after each step *via* CV in 10 mM $[Ru(NH_3)_6]Cl_3$/0.1 M KCl (3 consecutive cycles are shown, scan rate: 100 mV s^{-1}). (f) SEM image showing a cross section of the modified colloidal probe shown in (e); (g) EDX spectra recorded at the marked spots in f (red: core of the polystyrene sphere, blue: PEDOT:PSS, inset structure of PEDOT:PSS).

for the reduced polymer (Fig. 1g). PSS is a bulky counter anion, and for maintaining charge neutrality in the reduced state, cations (Na^+ ions) from the solution are incorporated into the polymer film.[28] Also the oxygen (O Kα) peak is higher for the PEDOT:PSS compared to the polystyrene colloid. The Ag Lα peak is related to the Ag component of the polystyrene colloid. Au is not visible because the film is significantly thinner. Raman spectroscopy was applied to further confirm the PEDOT:PSS deposition (Fig. S3†). Control experiments with respect to the potential-dependent adhesion behavior have been performed. As a test sample for measuring adhesion forces of the PEDOT:PSS-coated colloidal probe at different biases, a plasma-treated glass slide was chosen and serves as a model hydrophilic substrate, as demonstrated in previous similar experiments.[16] Measurements were conducted in 0.1 M KCl solution to screen electrostatic interactions. The order of applied potentials during measurements was as follows: −0.2 V (open circuit potential, OCP), followed by +0.8 V and −0.6 V *vs.* Ag/AgCl. The unbiased polymer-coated colloidal probe showed strong adhesive interactions with the surface OH groups of the glass slide with forces of 2.12 ± 0.53 nN (for all measurements, $N \geq 100$). Additionally, longer-range pulling forces are visible in the range of 10 to 50 nm (Fig. 2a). These rupture forces, which appear as a random sawtooth profile, are related to adhesion of several polymer chains and their subsequent stretching until they finally detach from the glass surface. When a positive potential was applied, the maximum adhesive interaction decreased to 1.58 ± 0.46 nN and significantly reduced rupture forces were observed. In this oxidized state, the interaction of a dopant with a positively charged polymer is higher due to ionic interactions with the immobile, anionic PSS^- dopant within the polymer matrix. Also, compared to the reduced state of the polymer, less sulfate groups from the dopant should be present at the surface. When applying a negative potential, the maximum adhesion rises again to 2.13 ± 0.53 nN, and the rupture forces were observed again, indicating that the polymer interaction can be reversibly switched. The oxidized polymer shows significantly less adhesion (the *t*-test was performed for statistical analysis; $p < 0.02$ was regarded as statistically significant). However, no significant difference in the adhesion forces was observed when comparing the applied negative potential (−0.6 V) and open circuit potential (−0.2 V) (Fig. 2b).

In the next step, the PEDOT:PSS colloidal AFM-SECM probes were used for single cell force spectroscopy measure-

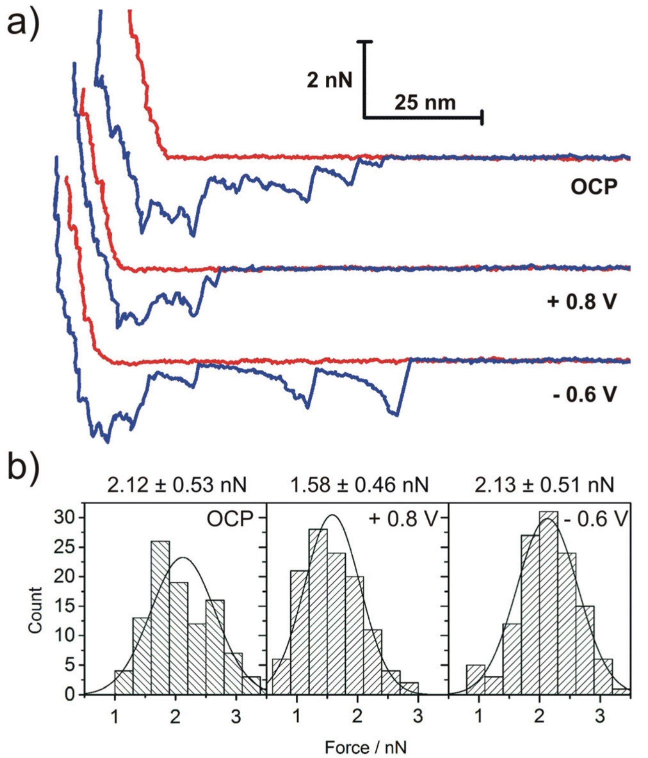

Fig. 2 Force spectroscopic measurements on a plasma-treated glass slide in 0.1 M KCl under potential control. (a) Typical force–distance curves obtained for the individual potentials (red = trace, blue = retrace) and (b) histograms of the measured maximum adhesion force ($N \geq 100$).

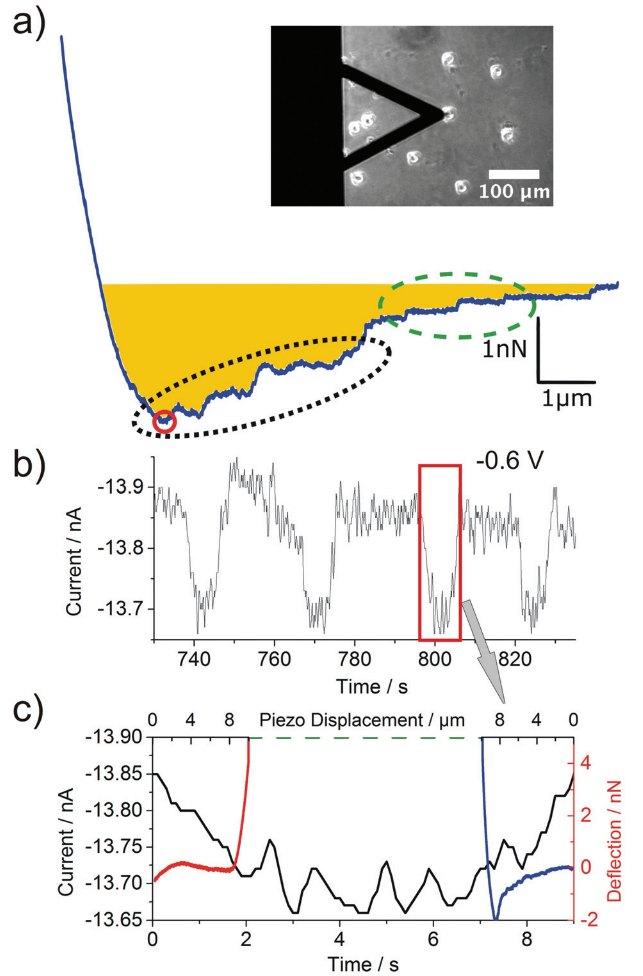

Fig. 3 Simultaneously obtained electrochemical data and force measurements. (a) Force curve (retract part) obtained at OCP on a fibroblast containing typical features known from SCFS (green-dashed marks membrane tethers, red-solid denotes the maximum force, black-dotted marks jumps and the yellow-shaded area reflects the obtained adhesion energy). The inset shows the AFM probe positioned above a single fibroblast cell with surrounding cells on the substrate. (b) Electrochemical response at −0.6 V, revealing a decrease in faradaic current during approach of the probe and at contact with the cell (≈ −13.7 nA) and (c) simultaneously obtained faradaic current (taken from boxed region in (b) and deflection signal *vs.* time and piezo displacement of a force curve recorded at a single cell.

ments. The adhesion between PEDOT:PSS and L929 mouse fibroblast cells was determined while applying potentials of −0.2 V (OCP), +0.8 V and −0.6 V *vs.* Ag/AgCl. A representative force curve obtained on a single cell at OCP is shown in Fig. 3a, with similar curves observed for bias voltages of +0.8 V and −0.6 V. For the OCP, the maximum force (red circle) and energy of adhesion (yellow area under curve) is 1.08 ± 0.41 nN and $2.13 \pm 0.85 \times 10^{-15}$ J, respectively. The curves also consisted of ruptures with forces of ≈50 pN, indicating molecular-level interactions associated with membrane tethers that are pulled away from the cell membrane (green-dashed mark) or cell surface molecules/receptors that remain anchored to the cell membrane–cytoskeleton complex (black-dotted region).[12] For the first time, local changes in electrochemical activity were simultaneously detected during force measurements on cells. With the probe biased at −0.6 V, a drop in current is observed when approaching the cells, leading to a plateau current in the contact area. Recovery of the current signal is evident during withdrawal of the probe (Fig. 3b and c). It is possible that a reduction of dissolved oxygen occurs at the PEDOT:PSS colloid and that during the approach and contact of the colloid with the cell, the diffusion of oxygen to its surface is hindered by the cell membrane (reflecting negative feedback current in the SECM experiment).[29] Alternatively, the consumption of oxygen by the living cell may result in the reduced current.[30] As the insulating glass substrate and the surrounding PPy (Fig. S4†) did not show a negative feedback, both effects may contribute to the current drop.

Histograms of the maximum energy and force as a function of the applied potential are shown in Fig. 4a and b. Surprisingly, neither the maximum energy nor the rupture forces and their interaction lengths as a function of the applied potential showed a statistically significant difference (Fig. 4c). Although, the length and force of the ruptures remain constant, more ruptures per curve were obtained at OCP.

In contrast, conventional SCFS studies combined with electrochemical-AFM have shown a significant increase in single cell adhesion on PPy doped with dodecylbenzene sulfo-

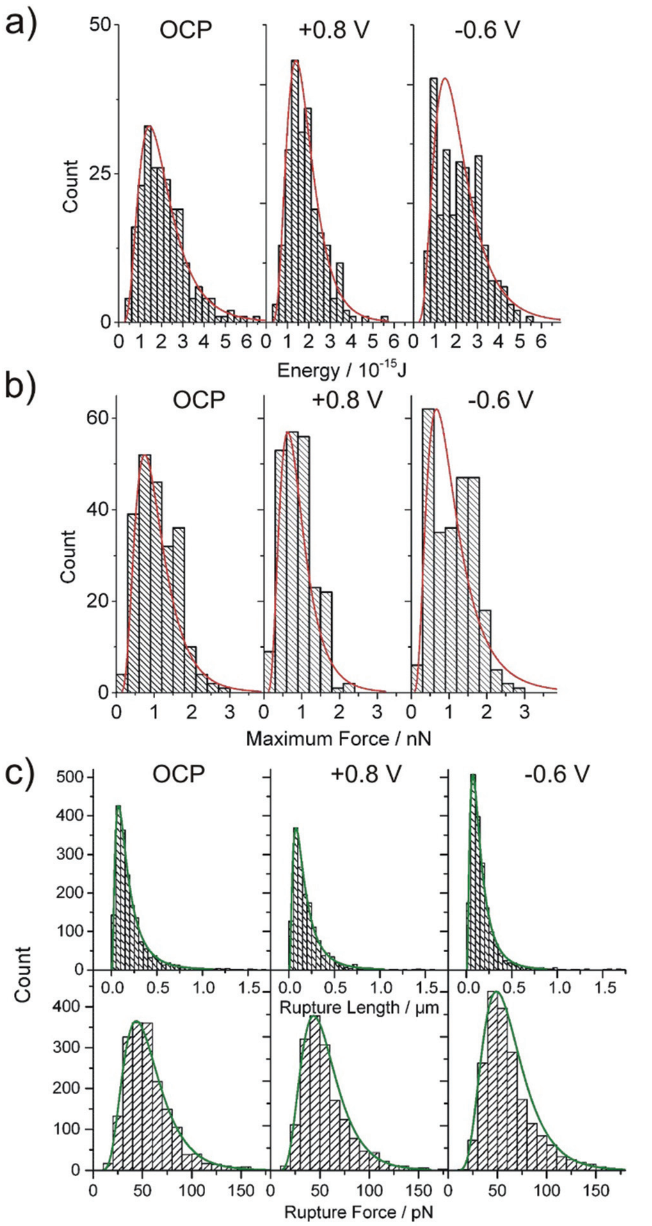

Fig. 4 Statistical data are shown in histograms for the different potentials (all *vs.* Ag/AgCl) (14 cells, 20 curves for each cell and potential). (a) Adhesion energy and (b) maximum force as a function of the potentials applied during measurement. Force spectroscopic rupture data (membrane tethers) recorded with PEDOT:PSS-coated colloidal AFM-SECM probes are shown in (c). Histograms are fitted with lognormal functions to obtain peak distribution values (14 cells, 20 curves for each cell and potential).

nate (PPy/DBSA) during electrically switching from the oxidized to the reduced state. In the reduced state (−800 mV), reorientation of DBSA sulfonate groups to the polymer surface and increased surface roughness, hydrophilicity and water uptake were observed, which contribute to the increased cell adhesion.[15] For PEDOT:PSS on the other hand, the PSS-dopant is a polymeric, anionic species (M_w = 70 000) with high chain length that is immobile and in excess at the polymer surface. Hence, electroneutrality in the reduced state is achieved by incorporating sodium ions from the solution and the overall polymeric structure does not drastically change, as demonstrated by spectroelectrochemical studies.[31] In comparison with the DBSA, these differences in the redox interactions of the PSS anion, may be responsible for the lack of dependence of cell adhesion on the applied potential. For the presented results, 10 cells were investigated with a single PEDOT:PSS-coated conductive colloidal AFM-SECM probe, and 4 cells were probed with two different probes to evaluate reproducibility of the measurements. Finally, after the cell measurements, a practical advantage of our approach is that the conductive colloid probes are reusable, as the colloid can be easily removed by dipping the cantilever in the piranha solution and a new conductive colloid can be attached to the exposed inlaid disc electrode, a procedure which can be performed in less than 30 minutes including the modification with the polymer layer.

Conclusions

"Conductive colloidal probe AFM-SECM" is an attractive approach for measurements at cell–material interfaces with high throughput, allowing improved statistical sampling of cells, and without the need of removing the examined cells from their substrate. The conductive colloids can be readily modified with various materials such as conductive polymers and applying a bias to the modified conductive colloidal probe facilitates understanding the effect of electrical signals on cell and molecular interactions. Uniquely, the force measurements may be performed simultaneously with localized electrochemical measurements for exploring the relationship between forces and electrochemical processes at biological interfaces.

Experimental

Probe fabrication

Commercially available NP-O probes (Bruker, Germany) were etched in aqua regia and buffered hydrogen fluoride solution to remove the reflective titanium/gold coating from the backside. A 5 nm titanium adhesion layer and a 95 nm gold layer were deposited onto the frontside using a shadow mask to coat a single cantilever, a connection path, and a contact pad on the chip. The frontside metal-coated cantilevers were then insulated with a mixed silicon nitride/dioxide film consisting of 10 alternating layers (total thickness: 1 µm) using PECVD.

The quality of the insulation was inspected with cyclic voltammetry. Afterwards an inlaid disc electrode was exposed using XeF_2-assisted FIB milling. A centered circular pattern (4 µm diameter) is milled into the frontside of the cantilever using insulator enhanced etching (IEE). With the endpoint monitor, milling was stopped right at the gold surface (Fig. S1b–d†). The exposed disc electrode is again characterized by CV.

The gold colloids (MicroParticles, Germany) were spread on a cleaned glass slide next to a small spot of Norland Optical Adhesive 81 (NOA 81, Norland Products, USA). The cantilever and the glass slide were mounted in the JPK NanoWizard II AFM (JPK, Germany) equipped with an inverted microscope. The probe was immersed into the UV-curable glue and several approaches to the bare glass slide were conducted to strip excess glue. As the used glue is not conductive, the gold colloid has to make direct contact with the underlying exposed gold layer. The cantilever was accurately positioned over the colloid and a manual approach was used for attaching the colloid. After curing the glue the contact between the conductive colloid and the gold electrode was confirmed *via* CV. When the cantilever was accurately positioned, the success rate of coming into contact with the colloid was 100%.

Electrochemical characterization and deposition

The electrochemical characterization of the fabrication steps was obtained in 10 mM $[Ru(NH_3)_6]Cl_3$/0.1 M KCl using a CHI 650d potentiostat (CH Instruments, USA) and the setup described in Fig. S2a,† inset. The contact pad of the cantilever chip is connected using a stainless steel clamp and the cantilever is immersed into the solution forming a convex meniscus (to avoid contact of the solution with the steel clamp or the contact pad) using a micromanipulator. The potential is cycled from 0.1 to −0.5 V (3 consecutive cycles) at a scan rate of 100 mV s^{-1}. For the PEDOT:PSS deposition, a degassed solution of 10 mM EDOT and 0.1 mM NaPSS was used. Dissolved oxygen was removed by purging all solutions with argon for 15 minutes. 10 CV cycles in a potential window of −0.6 V to 1 V (*vs.* Ag/AgCl; sat. KCl) at a scan rate of 100 mV s^{-1} were employed.

Force spectroscopic cell measurements

Force spectroscopy using the conductive colloidal probes was conducted in a cell incubator and the JPK electrochemistry cell (ECCell^{TM}) in a three-electrode setup, with the conductive colloidal probe as the working electrode, a Pt wire as the counter electrode and an Ag/AgCl reference electrode. Control measurements on plasma-treated glass were obtained in 0.1 M KCl with a loading force of 5 nN and a contact time of 2 s. The probe was mounted onto the holder and electrically connected. The insulation of the contact pad was carried out using insulation varnish. Prior to mounting the colloidal probe into the AFM, the cultured cells were injected, and allowed to seed onto the substrate (a PPy/DBSA-coated gold surface). CV was used to test the integrity of the insulation in the cell media. For all measurements, the spring constant of the cantilevers was determined with the thermal noise method. Force spectroscopy on cells was performed with a loading force of 5 nN and a contact time of 5 s and all measurements were conducted at 37 °C. A minimum of 10 force curves was recorded for each cell, with a resting period of 20 s between each curve. Force measurements were performed without applying a potential (which reflects the OCP), +0.8 V and −0.6 V (*vs.* Ag/AgCl).

FIB processing and HRSEM imaging were obtained with a Quanta 3D FEG or Helios Nanolab 600 instrument, respectively (FEI, Netherlands). All electrochemical measurements were conducted with a CH600 series potentiostat (CHI, USA). Raman spectra were recorded with a JY HR800 Spectrometer (Horiba, JPN).

Acknowledgements

The authors acknowledge the Boehringer Ingelheim Ulm University BioCenter (BIU), the German Federal Ministry of Education and Research (BMBF – NanoMatFutur: 13N12545) (Peter Knittel) for financial support. Also, the FIB Center UUlm at the Institute of Analytical and Bioanalytical Chemistry and the Cleanroom & Workshop at the University of Ulm are acknowledged for their assistance. The authors would also like to acknowledge the financial support from the China Scholarship Council (CSC) (Hongrui Zhang), ARC Australian Research Fellowship (A/Prof. Michael Higgins), ARC DP110104359 (A/Prof. Michael Higgins), Australian Academy of Science International Linkage Award (A/Prof. Michael Higgins & Dr Christine Kranz), ARC Laureate Fellowship (Prof. Gordon Wallace) and ARC Centre of Excellence for Electromaterials Science (ACES).

Notes and references

1 S. C. Luo, E. M. Ali, N. C. Tansil, H. H. Yu, S. Gao, E. A. B. Kantchev and J. Y. Ying, *Langmuir*, 2008, **24**, 8071–8077.
2 M. H. Bolin, K. Svennersten, X. Wang, I. S. Chronakis, A. Richter-Dahlfors, E. W. H. Jager and M. Berggren, *Sens. Actuators, B*, 2009, **142**, 451–456.
3 M. Marzocchi, I. Gualandi, M. Calienni, I. Zironi, E. Scavetta, G. Castellani and B. Fraboni, *ACS Appl. Mater. Interfaces*, 2015, **7**, 17993–18003.
4 W. L. Connors and J. Heino, *Anal. Biochem.*, 2005, **337**, 246–255.
5 H. Lu, L. Y. Koo, W. M. Wang, D. A. Lauffenburger, L. G. Griffith and K. F. Jensen, *Anal. Chem.*, 2004, **76**, 5257–5264.
6 E. A. Evans and D. A. Calderwood, *Science*, 2007, **316**, 1148–1153.
7 E. Evans, K. Ritchie and R. Merkel, *Biophys. J.*, 1995, **68**, 2580–2587.
8 R. I. Litvinov, H. Shuman, J. S. Bennett and J. W. Weisel, *Proc. Natl. Acad. Sci. U. S. A.*, 2002, **99**, 7426–7431.
9 K. C. Neuman and A. Nagy, *Nat. Methods*, 2008, **5**, 491–505.
10 M. Grandbois, W. Dettmann, M. Benoit and H. E. Gaub, *J. Histochem. Cytochem.*, 2000, **48**, 719–724.
11 M. Benoit, D. Gabriel, G. Gerisch and H. E. Gaub, *Nat. Cell Biol.*, 2000, **2**, 313–317.
12 J. Helenius, C.-P. Heisenberg, H. E. Gaub and D. J. Muller, *J. Cell Sci.*, 2008, **121**, 1785–1791.
13 J. Friedrichs, J. Helenius and D. J. Muller, *Nat. Protoc.*, 2010, **5**, 1353–1361.

14 P. Aliuos, A. Sen, U. Reich, W. Dempwolf, A. Warnecke, C. Hadler, T. Lenarz, H. Menzel and G. Reuter, *J. Biomed. Mater. Res., Part A*, 2014, **102**, 117–127.
15 H. Zhang, P. J. Molino, G. G. Wallace and M. J. Higgins, *Sci. Rep.*, 2015, **5**, 13334.
16 P. Knittel, M. J. Higgins and C. Kranz, *Nanoscale*, 2014, **6**, 2255–2260.
17 M. Kappl and H.-J. Butt, *Part. Part. Syst. Charact.*, 2002, **19**, 129.
18 P. Elter, T. Weihe, S. Bühler, J. Gimsa and U. Beck, *Colloids Surf., B*, 2012, **95**, 82–89.
19 G. Lanzani, *Nat. Mater.*, 2014, **13**, 775–776.
20 J. V. Macpherson and P. R. Unwin, *Anal. Chem.*, 2001, **73**, 550–557.
21 C. Kranz, G. Friedbacher, B. Mizaikoff, A. Lugstein, J. Smoliner and E. Bertagnolli, *Anal. Chem.*, 2001, **73**, 2491–2500.
22 J. Abbou, C. Demaille, M. Druet and J. Moiroux, *Anal. Chem.*, 2002, **74**, 6355–6363.
23 K.-H. Chung, J. R. Pratt and M. G. Reitsma, *Langmuir*, 2010, **26**, 1386–1394.
24 D. M. Schaefer, M. Carpenter, B. Gady, R. Reifenberger, L. P. Demejo and D. S. Rimai, *J. Adhes. Sci. Technol.*, 1995, **9**, 1049–1062.
25 D. Shoup and A. Szabo, *J. Electroanal. Chem. Interfacial Electrochem.*, 1982, **140**, 237–245.
26 A. J. Bard and L. R. Faulkner, *Electrochemical Methods - Fundamentals and Applications*, New York, 2nd edn, 2001.
27 V. S. Vasantha, R. Thangamuthu and S.-M. Chen, *Electroanalysis*, 2008, **20**, 1754–1759.
28 A. Michalska, A. Gałuszkiewicz, M. Ogonowska, M. Ocypa and K. Maksymiuk, *J. Solid State Electrochem.*, 2004, **8**, 381–389.
29 A. Bard, F. Fan, J. Kwak and O. Lev, *Anal. Chem.*, 1989, **138**, 132–138.
30 D. Zhan, X. Li, A. B. Nepomnyashchii, M. A. Alpuche-Aviles, F. R. F. Fan and A. J. Bard, *J. Electroanal. Chem.*, 2013, **688**, 61–68.
31 S. Sakamoto, M. Okumura, Z. Zhao and Y. Furukawa, *Chem. Phys. Lett.*, 2005, **412**, 395–398.